6th European Conference on Computational Mechanics (ECCM 6)
7th European Conference on Computational Fluid Dynamics (ECFD 7)
1115 June 2018, Glasgow, UK

ABSOLUTE INSTABILITY IN PLASMA JET

S. Demange[1], N. Kumar[2], M. Chiatto[3] and F. Pinna[4]

[1] von Karman Institute for fluid dynamics
Chausse de Waterloo 72, 1640, Rhode-Saint-Gense, Belgium
simon.demange@vki.ac.be, https://www.vki.ac.be

[2] Department of Process and Engineering, TU Delft
Leeghwaterstraat 39, 2628 CB Delft, The Netherlands
nishant.kumar@univ-poitiers.fr, https://www.tudelft.nl/3me/

[3] University of Naples Federico II
P.le Tecchio, 80, 80125 Napoli, Italy
matteo.chiatto@unina.it, http://www.dii.unina.it

[4] von Karman Institute for fluid dynamics
Chausse de Waterloo 72, 1640, Rhode-Saint-Gense, Belgium
fabio.pinna@vki.ac.be, https://www.vki.ac.be

Key words: Jet instabilities, Absolute Instabilities, Inductively Coupled Plasma wind tunnel, Linear Stability Theory

Summary. *Stability features of a plasma jet are investigated by means of Linear Stability Theory. The convective/absolute nature of the instabilities is determined by local spatio-temporal analyses of the impulse response of the flow for different stream-wise positions and different operative conditions. Frequencies, shapes and growth rate of the leading stability mode are compared to available experimental high speed camera recordings of the jet unsteadiness. The frequency range and mode shapes retrieved theoretically are in good agreement with the experimental results. However, the growth-rates of these modes indicate a fast transition to the turbulent regime which is not observed in the facility, which could be explained by non-parallel base flow or non-linear modal growth of the mode effects.*

1 INTRODUCTION

Understanding and predicting the atmospheric phenomena occurring during re-entry of manned capsules is still one of the most challenging issue of present day space exploration. Due to high orbital and entry velocities, the air in front of the objects approaching the earth is compressed, forming a bow shock through which pressure and temperature increase drastically until the air dissociates and reaches a plasma state in which the gases are ionized. To study such high enthalpy flows, the von Karman Institute operates since 1997 the most powerful Inductively Coupled Plasma wind tunnel in the world: the Plasmatron [1]. However, the phenomena studied in this facility, such as the ablation of Thermal Protection System materials and flow transition, are strongly coupled with the quality of the plasma jet blown into the test chamber, and the reproduction of conditions similar to atmospheric entry in the facility is eventually hampered by hydrodynamic instabilities of the jet, as observed by Cipullo et al. in [2] using high speed cameras.

The development and evolution of perturbations inside a jet were first presented by Michalke [5]. In particular, he described "[...] in a certain frequency range additional modes exist which may be called "irregular" [...]" [5], when a sufficient heating of the jet centerline was applied. Such a mode displayed a non-zero growth rate at nil frequencies, implying waves traveling upstream. In a later study by Huerre and Monkewitz [8] for planar shear layer, these modes were correlated with the concept of absolute instabilities, developed by Briggs and Bers [6, 7] for plasma physics. Since then, literature has shown the relevance of using the spatio-temporal formulation of the LST, assuming waves growing both in time and space, in order to distinguish between the *convective* and *absolute* instabilities. The absolute/convective nature of instabilities has been exhaustively studied for hot round jets, notably to improve aircraft propulsion performances. Monkewitz and Sohn in [9] showed that absolute instability arises in jet profiles with a density (or temperature) ratio under $S_e = \rho_c/\rho_\infty = 0.72$ at the nozzle exit. Furthermore, it showed that this ratio could be decreased by increasing the Mach number or the azimuthal mode number or by decreasing the velocity ratio. These results were later confirmed and extended by Lesshafft and Huerre [10], taking into account the full impulse response of the flow to highlight the competition between the convective and absolute instabilities at different group velocities. This study also showed that increasing viscosity would have a stabilizing effect for both types of instabilities. Interesting additional results were brought by the study of Balestra [11] in 2015 for coaxial heated jets, showing that with more complex profiles, new instability modes could appear and lower temperature ratios for which absolute instabilities lead the stability behavior.

Confinement effect on the convective/absolute transition of jet instability modes has been studied by Juniper in [12], and provided a complete methodology to identify valid saddle points. Centerline heating effects have also been studied for convective instabilities, introduced for supersonic jets by Luo and Sandham in [13], and more recently for viscous, compressible, subsonic jets by Gloor et al. [14].

However, to the author knowledge, all previous study of absolute instabilities with LST were considering perfect gases and profiles shapes far from the one met in the Plasma-

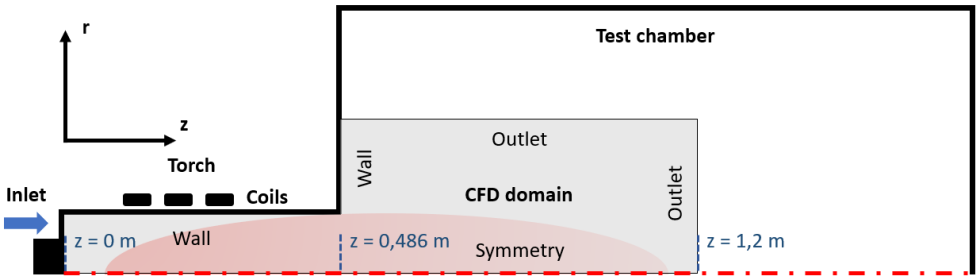

Figure 1: Sketch of the Plasmatron facility and CFD domain.

tron jet. The aim of this study is to compute the spatio-temporal impulse response of the Plasmatron jet for several stream-wise positions and power input to the facility and uncover the nature of the instabilities observed. The convective/absolute nature of the instabilities is first investigated, and compared to the experimental observations available in [2].

2 PROBLEM AND MODEL DESCRIPTION

2.1 Base flow

Plasmatron wind tunnel [1] creates a plasma jet by blowing air out of an annular inlet into a torch section, where it is heated by induction, up to ionization. It then enters the test chamber forming a hot jet as seen in Fig. 1. The base flow used for this study is obtained from two-dimensional axisymmetric CFD computations of the torch and test chamber using the open source code CoolFluid-ICP. This study will focus on high pressure cases for which the flow is close to thermodynamic and chemical equilibrium [15]. The CFD simulations are done assuming a ratio between the power inputted to the facility and the one received by the flow of $\eta = 0.5$; however, this value has never been formally confirmed. The first conditions studied in this paper correspond to the high pressure case from the study of Chiatto [4], assuming a power absorbed by to the flow of 90 kW, a static pressure of 20 kPa and an air flow rate of 16 g/s at the inlet. In section 3.4, the power is varied from $P_{el} = 80$ to 125 kW, while the other parameters are kept fixed. The high temperature effects and chemistry are taken into account in the CFD by using the Mutation++ library [15] for an 11 species air mixture. The computational domain is compared to a sketch of the facility in Fig. 1.

In order to minimize computational resources while obtaining smooth radial profiles of the physical quantities, analytical expressions are used to fit the CFD laminar base flow using the *fit* routine of MATLAB^{TM}. The derivatives of the profiles with respect to the radial coordinate are computed analytically. Stream-wise velocity and temperature profiles are obtained in the chamber section for a set of discrete stream-wise positions in a similar way than the one described by Chiatto in [4]. As the temperature outside the jet in the test chamber T_∞ is non zero, the fitted temperature profiles are corrected as follow: $T_{adim} = (T_{fit}(T_{ctr} - T_\infty) + T_\infty)/T_{ctr}$. One can note that using local fittings does not

retrieve a strictly smooth base flow along the stream-wise direction, therefore, a similar behavior is expected for stability features sensitive to the jet shape.
Remaining physical quantities are computed using the MUTATION++ library, assuming that pressure stays equal to the static pressure P_{tc} throughout the jet, and centerline quantities and the radius of the torch $L_{ref} = r_{torch} = 0.08$ m are used as reference for non-dimensionalization. More details about this procedure are given by Chiatto [4].

2.2 Linear Stability Theory

Once the base flow is obtained, the stability features of the jet are investigated using the local Linear Stability Theory expressed in cylindrical coordinates (z, r, θ), respectively the stream-wise, radial and azimuthal directions. The perturbations around the mean flow quantities (W, U, V, P, T), respectively the components of the velocity along (z, r, θ), the pressure and the temperature, are assumed to take the form of normal modes of the flow described as:

$$f'(z, r, \theta, t) = \hat{f}(r) e^{(i(\alpha z + m\theta - \omega t))} + c.c. \ , \tag{1}$$

Where α is the complex stream-wise wavenumber, q is the azimuthal integral wavenumber, ω is the complex angular frequency of the perturbation, and $\hat{f}(r)$ is the shape of the perturbation. Once the modal decomposition is applied to the linearized flow equations, the stability problem, with the appropriate boundary conditions can be reduced to an eigenvalue problem. Using the *temporal* formulation, that means imposing a real value of the wavenumbers α and q, one retrieves the associated complex frequency ω through a *dispersion relation* $\mathfrak{D}(\omega, q, k) = 0$. The ensemble of solutions to the *dispersion relation* is called spectrum of instabilities, and the mode with largest growth-rate ω_i leads the stability behavior of the flow. For each instability mode, the dimensional frequency can be retrieved from the real part of ω as $F = {}^{\omega_r W_{ctr}}/_{2\pi L_{ref}}$.
A first set of linearized compressible Navier-Stokes equations in cylindrical coordinates has been developed by Garcia Rubio in [3], and later completed by Chiatto in [4] including chemical reactions in equilibrium. The latter is used in this study. In both cases, the electro-magnetic terms have been neglected as their effects are mostly confined to the torch section of the Plasmatron.
As seen in Fig. 1, the CFD domain does not reach the physical outer wall of the test chamber, therefore the jet is not considered as confined. An open outer boundary condition is imposed for which all perturbation vanish. At the jet centerline, three distinct sets of compatibility and Dirichlet conditions are imposed depending on the desired value of the azimuthal integral wavenumber q.
Once the leading modes are identified for a given base flow, the spatio-temporal formulation is used to study the time asymptotic behavior of the jet instabilities at zero group velocity and uncover their absolute/convective nature. This formulation assumes a growth of the modes both in time and space, hence both the wavenumber α and frequency ω are complex. The convective/absolute nature of the instabilities is determined using the *Briggs-Bers criterion*, stating that the presence of a saddle point (here with subscript S) appearing in the contour of constant growth-rate ω_i in the complex wavenumber α

plane can be correlated with the presence of an absolute instability of the flow. However, a saddle point must be formed by the pinching of an α^+ and an α^- branch to be considered valid, in other words, by sufficiently increasing the value of ω_i on each side of the saddle point, one ω_i contour must lie in the $\alpha_i > 0$ upper plan and the other in the lower $\alpha_i < 0$ plan. The absolute instability found is then characterized by an *absolute frequency* ω_S and an *absolute wave-number* α_S, verifying $\frac{\partial \mathfrak{D}}{\partial \alpha}(\alpha_S, q, \omega_S) = 0$. At the saddle point, the *absolute growth-rate* $\omega_{i,S}$ determines the nature of the flow: if $\omega_{i,S} > 0$, the flow is absolutely unstable, and if $\omega_{i,S} < 0$, the flow is either convectively unstable or stable.

2.3 Numerical methods

The implementation of the linearized equations was performed by Rubio and Chiatto using the Derivation toolkit from the VKI Extensive Stability and Transition Analysis toolkit [16]. The stability computations are also performed using VESTA, calling the *eigs* routine from MATLAB$^{\text{TM}}$ to solve the *dispersion relation* over the numerical domain discretized using Chebyshev collocation points. The standard discretization is transformed using the TAN mapping technique developed by Bayliss and Turkel in [17], as it proved to be well suited for problems with thick shear layers.
The numerical tools used to find saddle points in the α complex plane and track their evolution along the stream-wise direction have first been developed by Kumar [18] for planar shear layers, and were adapted to cylindrical coordinates for the purpose of this study. The contour of the growth rate are obtained by using a *local* stability stability solver of VESTA and iterative method using the Newton-Raphson scheme is used to converge toward the saddle points [19].

3 RESULTS

3.1 Temporal stability of the plasma jet

The temporal stability study is performed for the jet obtained with $P_{el} = 90$kW, and for a set of discrete stream-wise positions in the test chamber. The number of collocation points is fixed to $N = 201$, as it is sufficient to reach an accuracy of two digits on the value of ω. In this study, it can be correlated with an error of the order of 2 Hz when considering reference velocities of order 10^2 m/s.
The integral azimuthal wavenumber q chosen for the stability computations is selected based on the following observation. The experimental study of Cipullo et al. [2] provides the normal variance distribution of the radiations recorded by high speed camera over the test chamber. Assuming that the perturbations recorded are due to hydrodynamic instabilities, these results can be correlated with the temperature eigenfunctions retrieved by the LST. As noticed by Chiatto in [4], for the case studied, the perturbations seems to be non zero at the centerline of the jet, which is only compatible to the centerline boundary conditions obtained for $q = 0$.
Sweepings over the real wavenumber α are performed for different values of q, at several stream-wise positions for the *leading* mode. The resulting curves of growth-rate and their associated frequencies are displayed in Fig. 2.

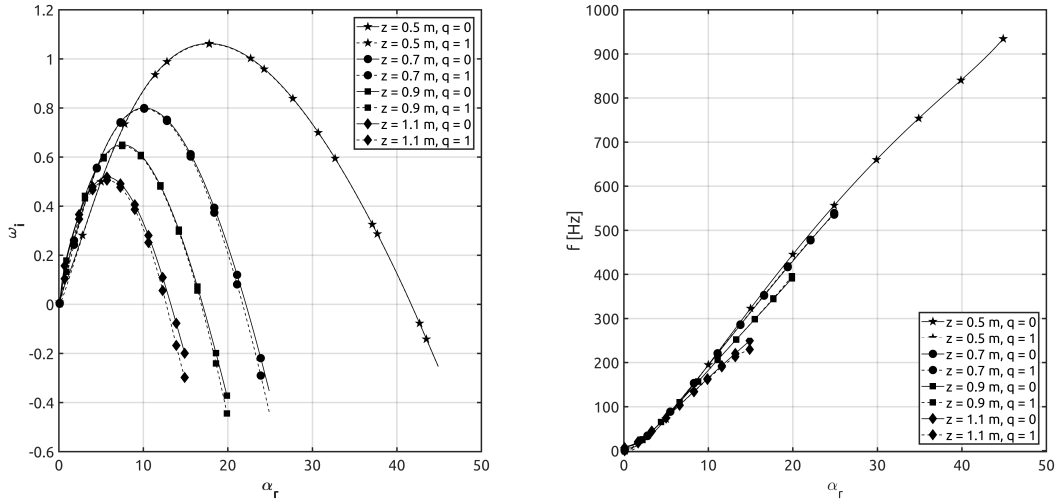

Figure 2: Growth-rate (left) and frequency (right) obtained from the sweeping over α_r for non-swirling (-) and swirling (- -) modes.

The behavior of the growth-rate curves with respect to the integral azimuthal wavenumber q is similar to the one described by Gloor in [14]. By increasing the value of q, the growth-rate is lowered for all frequencies. Therefore, axisymmetric modes dominate the stability behavior, and q is set to zero for the rest of this study.
The identification of the modes is done by observing the shape of the perturbation functions at the maximum amplification. The shapes are given in Fig. 3 for different stream-wise positions. The perturbations seem to retain the same overall shape along the stream-wise direction. Consistently, as the shear layer gets thicker while the jet is diffusing in the test chamber, so does the perturbations. However, the temperature perturbation features a peak around $r_{adim} = 0.25$ at the torch exit. This peak is found for $T = 8000$ K, where the temperature profiles displays an inflection point, which correspond to a hump in the profile due to the ionization. Such feature vanishes further downstream, as the centerline temperature of the jet decreases. Beside this observation, the shape of the modes are characteristic of the shear layer modes described by Lesshafft and Huerre in [10], displaying peaks at the shear layer center ($r_{adim} \simeq 1$). Similarly, the shape of the pressure function resembles the one of *inner* shear layer modes described by Gloor in [14] for co-flow jets. However, Gloor also describes the apparition of *outer* modes associated with the secondary part of the co-flow jet, prevailing at low frequencies, which are not observed here.

Flow parameters are given along the stream-wise positions in Tab. 1. One can note that the values of temperature ratio found in Plasmatron are one order of magnitude lower than for most flow studied in the literature ([10, 11, 14]), and that the flow is highly viscous. The maximum growth rate is found to decrease when the Reynold number and temperature ratio are increased, and when the Mach number is decreased. This behavior is different from the observations of Gloor for co-flow jets, which can originate from the

z(m)	M_{ctr}	Re	$S = {}^{T\infty}/_{T_{ctr}}$
0.5	0.036	117.5	0.035
0.7	0.030	131.7	0.047
0.9	0.028	149.4	0.052
1.1	0.027	162.8	0.055

Table 1: Main parameters at discrete stream-wise positions.

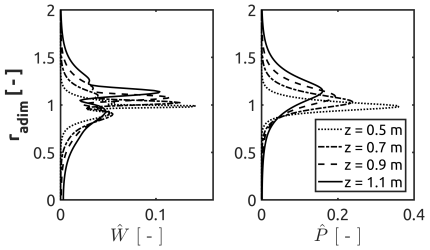

Figure 3: Perturbation functions for the set of stream-wise positions

range of parameters mentioned previously and the differences in the shapes of the profiles.

3.2 Local spatio-temporal analysis

The spatio-temporal analysis of the jet is carried out by computing the contours of constant growth-rate ω_i over the complex α plane. However, the size of the α plane to compute is case dependent, and for computations where large values of α must be considered to capture all the relevant saddle points, the computational effort can be considerable. With this in mind, a rule of thumb is applied to scale the required range of α_r used to produce the complex α plane: the size of the α plane is based on the values of α_r for which $\omega_i > 0$ during the temporal sweeping. According to this rule, the stream-wise position allowing to restrict the most the α plane is the last position in the test chamber, at $z = 1.1$ m. Once the contour plot is obtained for one stream-wise position and the saddles are identified, the saddles are tracked step by step in the stream-wise direction. The first contours of constant growth-rate at $z = 1.1$ m are displayed in Fig. 4a. As the spectrum obtained for a given α_{r1} and $-\alpha_{r1}$ are symmetrical, so are the contours with respect to the α_i axis. Therefore, only the half plan corresponding to positive α_r is computed.

Several saddle points are found over the α plane, noted from S_1 to S_6. Following the *Briggs-Bers criterion*, saddles lying on the upper half plane obtained for this study cannot be valid saddles, as no α^- branch crosses the α_r axis toward the upper plane. On the other hand, the saddle S_3 is pinched between an α^+ and an α^- branches, therefore it forms a valid saddle point at the location $\alpha_S = 0.475023$ - 0.726031i. Its associated real frequency is $\omega_{r,S} = 0.190295$ and *absolute growth-rate* is $\omega_{i,S} = 0.134455 > 0$. Given the sign of $\omega_{i,S}$, an absolute instability is found to develop at this stream-wise position.
The perturbation functions at the saddle are given in Fig. 4b. The pressure function is typical of a *mixed* mode described for single and co-flow jets, respectively by Lesshafft and Huerre in [10] and Balestra et al. in [11]. For these modes, the pressure perturbation is amplified both at the centerline and the shear layer. This can be explained as the α^+ and α^- branches pinching at the saddle display pressure perturbations respectively with the shape of shear layer and jet column modes. One can note that the temperature perturbations at the saddle are still in agreement with experimental observations given Fig. 9. Remaining saddle points S_4 to S_6 are formed between the pinching of the merged α^+ and α^- branches forming the saddle S_3 and a set of others α^- branches. Similarly

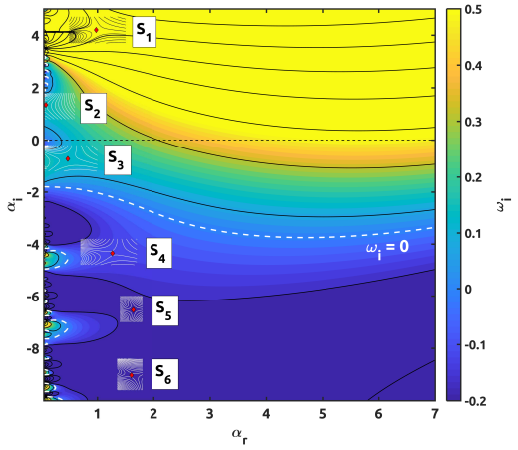

Figure 4(a): Contour of constant growth-rate ω_i obtained over the complex α plane for z =1.1 m.

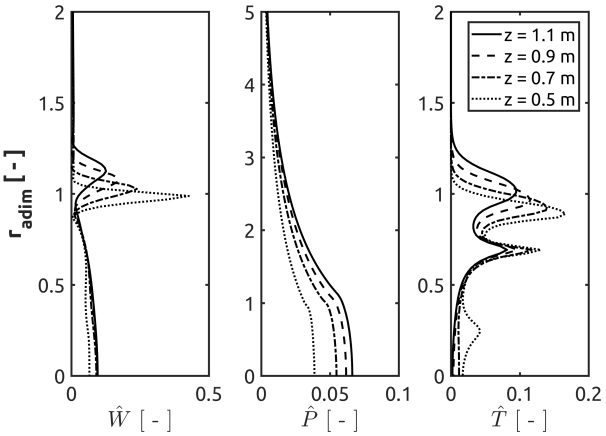

Figure 4(b): Perturbation functions for S_3 at the set of stream-wise positions.

to the study of Lesshafft and Huerre in [10], only the saddle point displaying the highest *absolute growth-rate* ω_{iS} is taken into account as it leads the stability behavior of the flow.

3.3 Influence of the stream-wise position

Once the spatio-temporal analysis is done for one stream-wise position, the saddles are tracked along the test chamber. This process is repeated iteratively for each stream-wise position with sufficiently small steps along z to allow the local solver to converge from a previous position. The accuracy of the tracking has been checked a posteriori by local spatio-temporal analyses around the supposed location of the saddle in the α plane, and the saddles were retrieved up to machine precision for ω_S and with an error of order 10^{-8} for α_S.

For this analysis, 25 stream-wise positions between 0.5 m and 1.1 m have been scanned, and only the valid saddles S_3 to S_6 are considered. The evolution of the growth-rates for each saddle are plotted in Fig. 5a. The saddle S_3 remains the leading one for the whole test chamber length, and its *absolute growth-rate* increases from $\omega_{i,z=0,5\mathrm{m}} = 0.0662$ to $\omega_{i,z=1,1\mathrm{m}} = 0.1344$ in the stream-wise direction. A first significant result is that the jet is found to be *absolutely unstable* for the whole test chamber length at the set of parameters studied. The evolution of the shape of the saddle point is plotted in Fig. 4b, and the mixed nature of the mode remains the same for all the chamber. Near the torch exit, the additional peak observed in the temperature function during the temporal sweeping is also present at the saddle. A second significant result is obtained when examining the *absolute frequency* along the stream-wise direction for the leading mode, displayed in Fig. 5b. One can note that the frequency plot retrieved by the tracking tool is particularly noisy, it has been associated with the stream-wise discontinuity between the locally fitted profiles, a cure for this phenomena would be to develop a global model of the jet, as done by Chiatto.

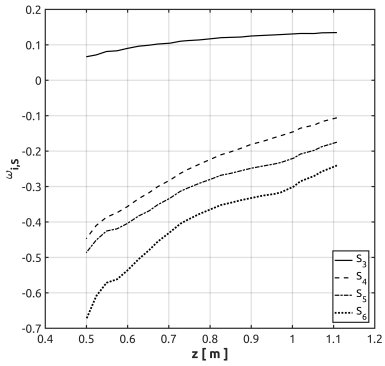

Figure 5(a): Evolution of saddle growth-rates along the stream-wise direction.

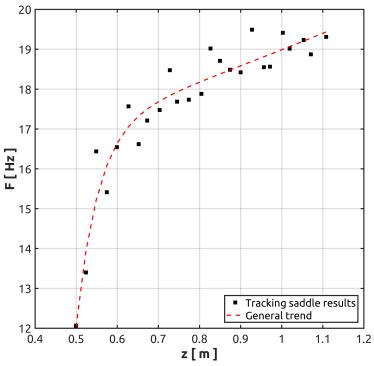

Figure 5(b): Evolution of *absolute frequency* of saddle S_1 along the stream-wise direction.

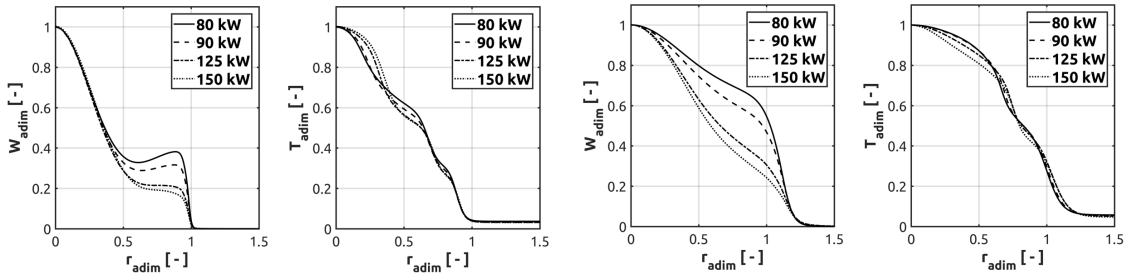

Figure 6: Influence of electric power on profiles at $z = 0.5$ m (left) and $z = 1.1$ m (right).

Nonetheless, this trend can still be compared against experimental results from Cipullo. Fig. 9 gives an indication of the most amplified frequencies in the flow. For the conditions studied, Cipullo indicates in [2] that the power rectifier delivers a frequency of 100 Hz. By comparing LST against experimental results, it seems that the instabilities are firstly dominated by the power rectifier at the torch exit. At this position, the growth-rate of the hydrodynamic instabilities is the lowest. Further downstream, the hydrodynamic instabilities (around 20 Hz) seem to dominate the stability behavior of the flow, which could be due to their larger growth-rate. One can also note that, due to the lack of precision in the experimental evolution of the frequency, the current comparison is only qualitative.

3.4 Influence of the electric power

The procedure described in previous sections is applied for base flows computed at different electric powers, respectively $P_{el} = 80, 90, 125$ and 150 kW. The new non-dimensional profiles are displayed Fig. 6. The power rise makes the profiles sharper, and increases the centerline quantities as seen in Tab. 2.

The topology of the constant ω_i contours in the complex α plane at the different electric powers, however, remains similar to the one displayed Fig. 4a. A saddle similar to S_3 found

in section 3.2 is observed for each power, and remains the leading saddle point over the parametric (P_{el}, z) plane. The tracking of the saddle along the stream-wise direction is carried out, and the results are presented Fig. 7. For all powers, the behavior of the saddle in the stream-wise direction is similar to the $P_{el} = 90$ kW case, hinting that the same physical phenomena are leading the stability behavior for all power studied. As noticed previously, the $\omega_r(z)$ curves obtained are noisy, displaying a greater sensitivity of ω_r to the base flow than ω_i. For all power studied, the nature and shape of the mode at the saddle points are similar, with the differences in shape being caused by the sharpening of the jet due to an increased power.

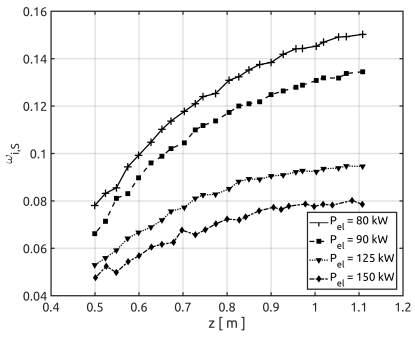

Figure 7: Evolution of $\omega_{i,S}$ along the stream-wise direction for $P_{el} = 80, 90, 125$ and 150 kW.

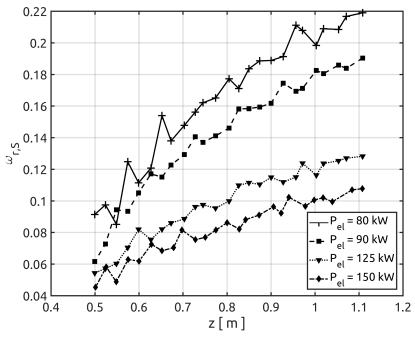

Figure 8: Evolution of $\omega_{r,S}$ along the stream-wise direction for $P_{el} = 80, 90, 125$ and 150 kW.

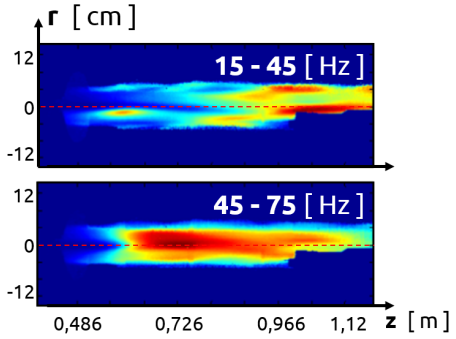

Figure 9: Partial power distributions for $P_{el} = 200$ kW and $P_{tc} = 20$ kPa from [2].

The frequencies are retrieved from LST computations for each power, and their maximum along the stream-wise direction are compared to *global* frequencies obtained experimentally by Cipullo [2] in Tab. 2. Based on the behavior of ω_r along z, one can make the assumption that the maximum frequency is representative of the frequencies amplified in the second half of the test chamber.

P_{el}(kW)	F_{exp}(Hz)	F_{LST}(Hz)	$W_{c,z=0\ 5m}$(m/s)	$T_{c,z=0\ 5m}$(K)
80	20	19.3	80.84	9547
90	20	19.45	98.54	10111
125	30	21.47	154.88	11033
150	45	23.13	187.46	11331

Table 2: Comparison of frequencies retrieved experimentally and from LST.

Results from the LST and global experimental frequency seem to agree for low powers setups ($P_{el} = 80$ and 90 kW). However, this is not the case for higher values of power. Such difference can have different explanations. Firstly, the global frequency observed experimentally might not correspond to the local one found with the local LST. Juniper

in [12] showed that local absolute instabilities could trigger global instabilities, however the frequency of such global instability could be different from the local one retrieved in this study. Differences may also come from CFD base flow computations, current CFD results should be compared to another code simulations handling high temperature effects. Furthermore, Cipullo hints that the main contribution to the change of hydrodynamic frequency comes from static pressure in the chamber rather than power.

4 CONCLUSIONS

A local spatio-temporal analysis of the plasma jet developing in the VKI Plasmatron test chamber was performed using the Linear Stability Theory on analytical profiles fitted to CFD simulations. The analysis for $P_{el} = 90$ kW revealed the presence of an absolute instability at the end of the test chamber ($z = 1.1$ m) with an *absolute frequency* of 19.23 Hz, coherent with experimental observations of Cipullo. The absolute instability displays the characteristic shape of a mixed jet column/shear layer mode, also observed by Balestra in co-flow jets. A tracking tool has been used to study the evolution of the absolute instability along the stream-wise direction, revealing that the absolute frequency and growth rate increase with the position in the test chamber. By comparing these results with experimental observations of Cipullo, a possible mechanism at play in the instability behavior of the facility has been proposed: at the torch exit, the flow is dominated by the instabilities of the facility power rectifier, while when increasing the stream-wise position, the hydrodynamic instabilities dominate the flow behavior with lower frequencies. Similar stability computations have been performed for a range of power returning coherent results coherent with the experimental observations for low powers($P_{el} = 80$ and 90 kW). Finally, the local LST does not match the global experimental results for higher powers, hinting to a possible rise of a global mode of different frequency.

5 ACKNOWLEDGMENT

This work was supported by the Fonds de la Recherche Scientifique - FNRS under the FRIA Grant.

REFERENCES

[1] Bottin, B. and Carbonaro, M. and Van Der Haegen, V. and Novelli, A. and Vennemann, D. *The VKI 1.2* MW *Plasmatron facility for the thermal testing of TPS materials*. 3 rd European Workshop on Thermal Protection Systems, ESTEC, 1998.

[2] Cipullo, A. and Helber, B. and Panerai, F. and Zeni, F. and Chazot, O. *Investigation of freestream plasma flow produced by inductively coupled plasma wind tunnel*. Journal of Thermophysics and Heat Transfer, Vol 28, No 3, pp 381–393, 2014.

[3] Garcia Rubio, F. *Numerical study of plasma jet unsteadiness for re-entry simulation in ground based facilities*. von Karman Institute for fluid dynamics, 2013.

[4] Chiatto, M. *Numerical study of plasma jets by means of linear stability theory*. von Karman Institute for fluid dynamics, 2014.

[5] Michalke, A. *Survey on jet instability theory*. Progress in Aerospace Sciences, Vol 21, pp 159–199, 1984.

[6] Briggs, R. *Electron-stream interaction with plasmas*. M.I.T. Press, 1964.

[7] Bers, A. *Space-time evolution of plasma instabilities-absolute and convective*. Basic Plasma Physics: Selected Chapters, Handbook of Plasma Physics, Volume 1, p 451, 1984.

[8] Huerre, P. and Monkewitz, P. A. *Absolute and convective instabilities in free shear layers*. Journal of Fluid Mechanics, Vol 159, pp 151–168, 1985.

[9] Monkewitz, P. and Sohn, K. *Absolute instability in hot jets and their control*. 10th Aeroacoustics Conference, American Institute of Aeronautics and Astronautics, 1986.

[10] Lesshafft, L. and Huerre, P. *Linear impulse response in hot round jets*. Physics of Fluids, Vol 19, No 2, 2007.

[11] Balestra, G. and Gloor, M. and Kleiser, L. *Absolute and convective instabilities of heated coaxial jet flow*. Physics of Fluids, Vol 27, No 5, 2015.

[12] Juniper, M. *The effect of confinement on the stability of non-swirling round jet/wake flows*. Journal of Fluid Mechanics, Vol 605, pp 227–252, 2008.

[13] Luo, K. H. and Sandham, N. D. *Instability of vortical and acoustic modes in supersonic round jets*. Physics of Fluids, Vol 9, No 4, pp 1003–1013, 1997.

[14] Gloor, M. and Obrist, D. and Kleiser, L. *Linear stability and acoustic characteristics of compressible, viscous, subsonic coaxial jet flow*. Physics of Fluids, Vol 25, No 8, pp 084102, 2013.

[15] Magin, T. and Degrez, G. *Transport Algorithms for Partially Ionized and Unmagnetized Plasmas*. Journal of computational physics, Vol 198, No 2, pp 424–449, 2004.

[16] Pinna, F. *Numerical Study of Stability For Flows from Low to High Mach Number*. PhD Thesis, von Karman Institute for fluid dynamics, 2012.

[17] Bayliss, A. and Turkel, E. *Mappings and accuracy for Chebyshev pseudo-spectral approximations*. Journal of Computational Physics, Vol 101, No 2, pp 349–359, 1992.

[18] Kumar, N. *Spatio temporal stability of shear layers*. von Karman Institute for fluid dynamics, 2017.

[19] Rees, S. J. *Hydrodynamic instability of confined jets wakes implications for gas turbine fuel injectors*. PhD Dissertation, Department of Engineering, University of Cambridge, 2008.